frontiers | Frontiers in Membrane Science and Technology

TYPE Original Research
PUBLISHED 06 February 2024
DOI 10.3389/frmst.2024.1355773

OPEN ACCESS

EDITED BY
Yunxia Hu,
Tianjin Polytechnic University, China

REVIEWED BY
Xiaobin Yang,
Harbin Institute of Technology, China
Chuanjie Fang,
Zhejiang University, China

*CORRESPONDENCE
Shoujian Gao,
sjgao2012@sinano.ac.cn
Jian Jin,
jjin@suda.edu.cn

RECEIVED 14 December 2023
ACCEPTED 23 January 2024
PUBLISHED 06 February 2024

CITATION
Gao S, Liu P and Jin J (2024), *In-situ* ionized construction of PVDF/sodium polyacrylate-grafted-PVDF blend ultrafiltration membrane with stable anti-oil-fouling ability for efficient oil-in-water emulsion separation.
Front. Membr. Sci. Technol. 3:1355773.
doi: 10.3389/frmst.2024.1355773

In-situ ionized construction of PVDF/sodium polyacrylate-grafted-PVDF blend ultrafiltration membrane with stable anti-oil-fouling ability for efficient oil-in-water emulsion separation

Shoujian Gao[1]*, Pingping Liu[2] and Jian Jin[3]*

[1]i-Lab, CAS Key Laboratory of Nano-Bio Interface, Suzhou Institute of Nano-Tech and Nano-Bionics, Chinese Academy of Sciences, Suzhou, China, [2]Nano Science and Technology Institute, University of Science and Technology of China, Suzhou, China, [3]College of Chemistry, Chemical Engineering and Materials Science, Collaborative Innovation Center of Suzhou Nano Science and Technology, Soochow University, Suzhou, China

Traditional polymeric membranes usually suffer from serious oil fouling and quick decline of water flux when separating oil-in-water emulsions. In this work, we report the fabrication of the sodium polyacrylate (PAAS) blended polyvinylidene fluoride (PVDF) ultrafiltration membrane which behaves hydrophilicity, underwater low-oil-adhesive superoleophobicity and outstanding anti-oil-fouling ability even for viscous crude oil. The blend membrane was fabricated via a two-step method, including the nonsolvent-induced phase inversion of PVDF/polyacrylic acid-grafted-PVDF (PVDF/PAA-g-PVDF) blend membrane and the subsequent *in-situ* ionization of PAA into PAAS. The two-step method improves the affinity between the strong hydrophilic additive PAAS and the hydrophobic polymer matrix PVDF, thus endowing the blend membrane with long-term stable superwetting property for 1,100 days. The PVDF/PAAS-g-PVDF blend membrane can efficiently separate multiple emulsifier-stabilized oil-in-water emulsions with ultrahigh separation efficiency of 99.97% (the residual oil content in the filtrate is lower than 3 ppm after one-step separation) and high water flux of 350 L m^{-2} h^{-1} bar^{-1}. The blend membrane also shows good cycling performance, and can be easily cleaned by water washing during several separation cycles of the crude oil-in-water emulsion. This work inspires a feasible route of fabricating stable anti-oil-fouling membranes for separation of emulsified oily water.

KEYWORDS

blend membrane, anti-oil-fouling, *in-situ* ionization, oil/water separation, oil-inwater emulsion

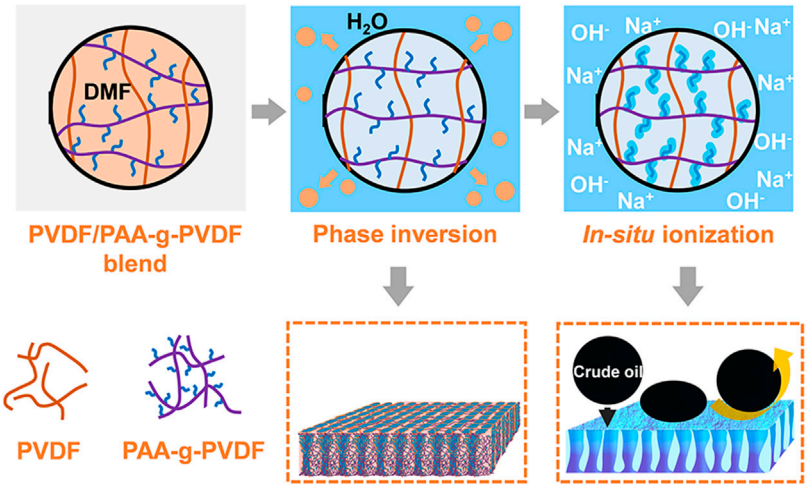

GRAPHICAL ABSTRACT

1 Introduction

Oily water generated from diverse oil-related activities such as oil recovery, petrochemical, metal finishing, food and leather industries has become a serious pollution problem around the world (Gao et al., 2015; Wang et al., 2023). It harms both the environment and human health (Oki and Kanae, 2006; Aurell and Gullett, 2010). Separating oil from oily water is recognized as a sustainable strategy, and has been extensively studied (Chu et al., 2015; Wang et al., 2015). However, long-term efficient separation of oil-in-water emulsions with the oil droplet size at a micro- or nanometer scale is still challenging. Membrane separation is an efficient technology for separating the oil-in-water emulsions due to its high efficiency, ease of operation and low energy consumption (Elimelech and Phillip, 2011; Chang et al., 2014). An obstacle of traditional membranes for separating oil-in-water emulsions is that the water flux declines quickly because of inevitable oil fouling on the membrane surfaces, which limits the separation capacity and long-term use of the membranes (Rana and Matsuura, 2010; Yang et al., 2022). The oil fouling is particularly serious during the separation of crude oil-in-water emulsion due to the high oil viscosity (Gao et al., 2022). So far, developing advanced membranes with an outstanding anti-oil-fouling property for efficient and long-term stable separation of oil-in-water emulsions remains highly desired.

Generally, hydrophilic membranes can form hydration layers on their surfaces in water and protect the membranes from oil fouling (Gao et al., 2015; Dong et al., 2022). Surface grafting and surface coating are effective techniques for fabricating the hydrophilic membranes, but they usually have the drawbacks of time consumption, harsh chemical environment requirement and coating layer instability. (Zhang et al., 2013a; Chen and Xu, 2013; Yang et al., 2014; Gao et al., 2015). Recently, the strategies for building biomimetic coatings with mild and versatile merits, as well as the atomic layers with precise and controllable features raise an exciting opportunity for fabricating the hydrophilic and anti-oil-fouling membranes (Yang et al., 2021; Geng et al., 2022; Yang et al., 2023). These approaches represent the state-of-the-art technologies in surface modification, but still have a long way to go before industrialization. The interfacial energy and wettability difference of oil and water on solid surfaces provide another brand-new route for constructing the superhydrophilic and underwater superoleophobic membranes with high-surface-energy membrane materials and surface micro-/nanostructures (Zhang et al., 2013b; Tao et al., 2014; Zhang et al., 2014). But, it is difficult to construct micro-/nanostructures on polymeric membrane surfaces via common membrane-manufacturing methods. Blending hydrophilic additives like hydrophilic polymers, amphiphilic copolymers and inorganic nanoparticles, etc., In the traditional membrane matrixes like polyvinylidene fluoride (PVDF), polysulfone and polyether sulfone, etc., Through the phase inversion is widely adopted for fabricating the hydrophilic and anti-oil-fouling polymeric membranes (Shi et al., 2008; Liu et al., 2011; Kang and Cao, 2014; Chen et al., 2016). Compared with other techniques, blending modification is ease of operation and scaling up for industrialization. Nevertheless, the polarity difference and the weak interaction between the hydrophilic additives and the hydrophobic polymer matrixes often lead to the aggregation of the hydrophilic additives during the phase inversion. It finally brings about the non-uniform distribution and the easy release of the hydrophilic additives from the blend membranes (Choi et al., 2006; Zhu et al., 2014). Blending strong hydrophilic additives in traditional hydrophobic polymer matrixes to fabricate uniform and long-term stable membranes with hydrophilicity and superior anti-oil-fouling property is still a tough work.

Herein, we propose a two-step method to uniformly introduce a strong hydrophilic additive sodium polyacrylate (PAAS) in the hydrophobic PVDF and construct a hydrophilic, underwater superoleophobic and anti-oil-fouling blend membrane. PAAS is a well-known hydrogel material with underwater low-oil-adhesive superoleophobicity and superior anti-oil-fouling property even for viscous oils (Gao et al., 2016). But, it is difficult to directly blend PAAS with the hydrophobic polymer matrixes to obtain uniform and stable membranes. In our method, polyacrylic acid-grafted-PVDF (PAA-g-PVDF) was chosen as an additive precursor to blend with PVDF and form a PVDF/PAA-g-PVDF blend membrane via the nonsolvent-induced phase inversion (Figure 1). Then the PVDF/PAA-g-PVDF blend membrane was

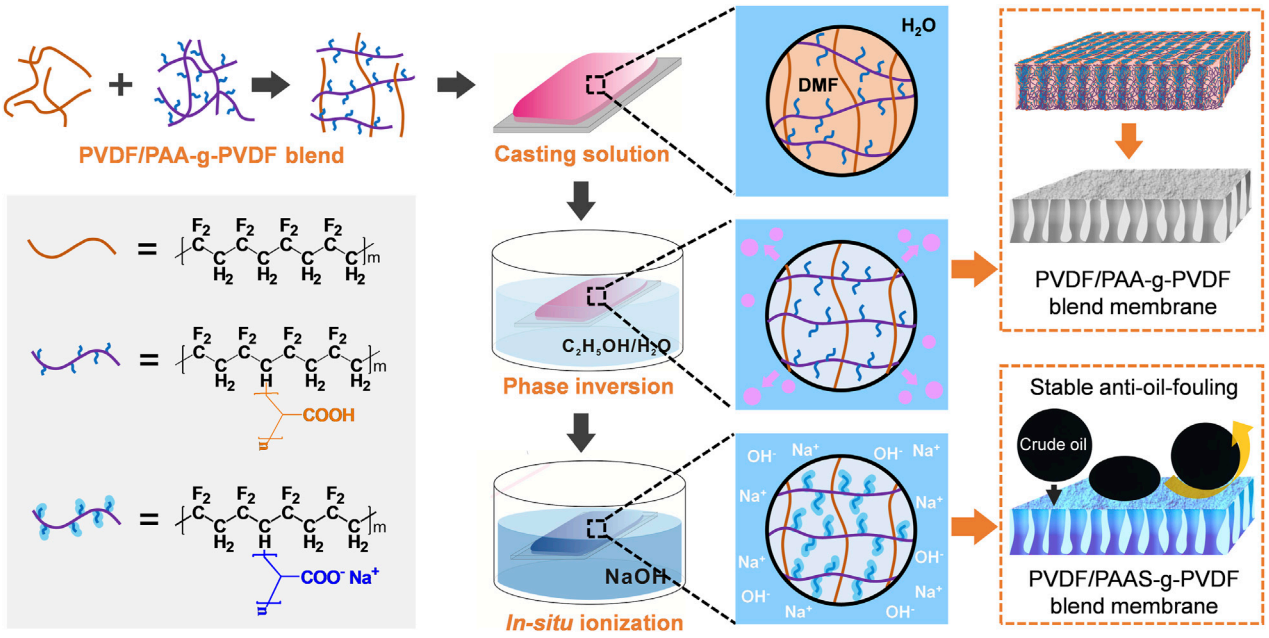

FIGURE 1
Schematic illustration for the fabrication of the anti-oil-fouling PVDF/PAAS-g-PVDF blend membrane.

treated by NaOH solution where PAA was *in situ* ionized to PAAS, and the PVDF/PAAS-PVDF blend membrane was fabricated. The two-step method improves the affinity between PAAS and PVDF, thus endowing the blend membrane with good uniformity and stable superwetting property. The wettability and water permeation flux of the PVDF/PAAS-g-PVDF blend membrane is controllable by regulating the mass ratio of PAA-g-PVDF and PVDF. The blend membrane can achieve efficient separation of multiple emulsifier-stabilized oil-in-water emulsions with ultrahigh separation efficiency of 99.97%, high water flux of 350 L m^{-2} h^{-1} bar^{-1}, as well as good cycling performance even for the crude oil-in-water emulsion.

2 Material and methods

2.1 Materials

PVDF powders (Solvay, Solef 1015, Mn = 238000) used in this work were purchased from Solvay Chemicals Company. PAA-g-PVDF powders with 8 wt% PAA graft ratio was synthesized via a pre-irradiation induced graft polymerization technique (45). Light crude oil (API Gravity >20°) and heavy crude oil (API Gravity: 10°–20°) were supplied by SINOPEC SABIC Tianjin Petrochemical Co., Ltd., China. Light crude oil was used for the separation of oil-in-water emulsion, and heavy crude oil was used for the measurement of oil contact angle (CA) and oil adhesive force. Diesel oil and soybean oil were commercial products from market. All other chemicals were commercially available from Shanghai Chemical Reagent Co. Ltd., and used as received without further purification. Deionized water was used throughout the experiments.

2.2 Preparation of the PVDF/PAAS-g-PVDF blend membrane

The PVDF/PAAS-g-PVDF blend membrane was prepared via the nonsolvent-induced phase inversion and the alkaline-induced *in-situ* ionization. PVDF/PAA-g-PVDF mixed powders with the PAA-g-PVDF: PVDF mass ratios of 3: 1, 2: 1, 1: 1, 1: 2 and 1: 3 were prepared, respectively. 3.6 g PVDF/PAA-g-PVDF mixed powders were dissolved in 32.4 g N, N′-dimethylformamide (DMF) to form the homogeneous solution under 85°C for 48 h. The solution was casted onto a flat glass plate by a casting knife with a gate height of 200 μm and then immersed in the water/ethanol (volume ratio = 1: 1) coagulation solution immediately. After 12 h, the PVDF/PAA-g-PVDF blend membrane was obtained. Then the PVDF/PAA-g-PVDF blend membrane was immersed in the 0.1 mol L^{-1} NaOH solution for 1 min. During this process, PAA reacted with NaOH and transformed into PAAS *in situ*. The PVDF/PAAS-g-PVDF blend membrane was thus obtained and then rinsed with water.

2.3 Separation of the oil-in-water emulsions

Three emulsifier-stabilized oil-in-water emulsions were prepared by mixing and stirring oil (soybean oil, diesel oil and crude oil) and water with an oil/water volume ratio of 1: 99, respectively. 0.1 mg mL^{-1} sodium dodecyl sulfate (SDS) was used as the emulsifier and added in water to prepare the oil-in-water emulsions. The soybean oil-in-water and diesel oil-in-water emulsions were prepared under stirring at a speed of 2000 rpm for 2 h. The crude oil-in-water emulsion was prepared under stirring at a speed of 8,000 rpm for 6 h. The PVDF/PAAS-g-PVDF blend membrane was fixed in a membrane cell with an effective filtration area of 7.06 cm^2. The separation process was carried out under

a cross-flow filtration mode. The membrane was firstly compacted by pure water under a transmembrane pressure of 1 bar for 30 min. Then 50 mL SDS-stabilized oil-in-water emulsion was filtrated through the membrane under 1 bar. The filtrated water was collected, and the oil content in the filtrate was determined by a TOC analyzer. Water flux J (L m^{-2} h^{-1} bar^{-1}) of the membrane was calculated according to Eq. 1:

$$J = \frac{\Delta V}{A\Delta t} \tag{1}$$

where ΔV was the volume (L) of filtrated water through the membrane, Δt is the filtration time (h), and A is the effective filtration area (m^2).

Separation efficiency E (%) of the oil-in-water emulsion was calculated according to Eq. 2:

$$E = \left(1 - \frac{C_1}{C_0}\right) \times 100\% \tag{2}$$

where C_1 and C_0 was the oil content in the filtrate and the emulsion feed, respectively.

2.4 Evaluation of the antifouling and cycling performance

To evaluate the antifouling and cycling performance of the membrane, three separation cycles of the SDS-stabilized crude oil-in-water emulsion were carried out, and the water flux was monitored in real time. In each separation cycle, pure water was firstly filtrated though the membrane under 1 bar for 30 min, and the stabilized water flux was recorded as J_{w1} (L m^{-2} h^{-1} bar^{-1}). Then the SDS-stabilized crude oil-in-water emulsion was filtrated through the membrane under 1 bar for 60 min, and stabilized water flux was recorded as J_{p1} (L m^{-2} h^{-1} bar^{-1}). Then the membrane was washed by hydraulic flushing for 30 min to complete one cycle. After water washing, pure water flux of the membrane was re-measured and recorded as J_{w2} (L m^{-2} h^{-1} bar^{-1}). Flux decline ratio (DR, %) and flux recovery ratio (FRR, %) were calculated according to the following equations, respectively:

$$DR = \left(1 - \frac{J_p}{J_{w1}}\right) \times 100\% \tag{3}$$

$$FRR = \frac{J_{w2}}{J_{w1}} \times 100\% \tag{4}$$

Reversible fouling ratio (Rr, %) and irreversible fouling ratio (Rir, %) were calculated according to the following equations, respectively:

$$R_r\,(\%) = \frac{J_{w2} - J_{P1}}{J_{w1}} \times 100\% \tag{5}$$

$$R_{ir}\,(\%) = \frac{J_{w1} - J_{w2}}{J_{w1}} \times 100\% \tag{6}$$

2.5 Evaluation of the long-term stability

Several PVDF/PAAS-g-PVDF blend membranes were cut into 100 pieces of square membranes with a size of 4 cm × 4 cm. The membranes were immersed in water with the pH of about 7. Every 15 days, a piece of the membrane was taken and washed by hydraulic cleaning for 30 min, then the measurements of water CA, underwater crude oil CA and underwater crude oil adhesive force were carried out on the membrane. Meanwhile, the water socking the membranes was replaced with new water every 15 days. The water CA, underwater crude oil CA and underwater crude oil adhesive force of the membranes were recorded for 1,100 days.

2.6 Characterization

Scanning electron microscopy (SEM) images and energy dispersive x-ray (EDX) spectrum were obtained on a Quanta FEG 250 SEM (FEI, America). Attenuated total reflectance Fourier transform infrared spectroscopy (ATR-FTIR) was measured by a Nicolet 6700 FTIR spectrometer (Nicolet, America). Water CA and underwater oil CA were measured on an OCA20 machine (Data-physics, Germany). Underwater oil-adhesive force was measured by a DCAT11 high-sensitivity micro-electro-mechanical balance system (Data-Physics, Germany). Tensile strength was determined on an Instron 3,300 universal testing machine (Instron, America). Oil and polyethylene glycol (PEG) contents in water were determined by an Aurora 1030w total organic carbon (TOC) analyzer (O.I. Analytical, America).

3 Results and discussion

3.1 Fabrication and morphology characterization of the blend membrane

As shown in Figure 1, the PVDF/PAAS-g-PVDF blend membrane was fabricated via the nonsolvent-induced phase inversion of the PVDF/PAA-g-PVDF blend membrane and the subsequent *in-situ* ionization of PAA into PAAS. Compared with the strong hydrophilic PAAS, PAA-g-PVDF has better compatibility with the hydrophobic PVDF. Therefore, blending PAA-g-PVDF with PVDF can relieve the aggregation of the additive during the phase inversion and form a more homogeneous blend membrane than directly blending PAAS with PVDF. After PAA transformed into PAAS *in situ*, the PVDF/PAAS-g-PVDF blend membrane with a uniform distribution of PAAS was obtained. Meanwhile, PAAS-g-PVDF has relatively strong interaction with PVDF, thus reducing the release of the additive into water and endowing the PVDF/PAAS-g-PVDF blend membrane with high stability for long-term use. It is worth noting that the pure PAAS-g-PVDF membrane is hardly permeable despite the membrane behaves a hydrophilic and anti-oil-fouling property, because the easy hydrating and swelling feature of PAAS blocks the membrane pores.

Figure 2 reveals the morphology and chemical composition of the PVDF/PAAS-g-PVDF blend membrane which is fabricated with the PVDF: PAA-g-PVDF mass ratio of 2: 1. The top-view SEM image of the dry PVDF/PAAS-g-PVDF blend membrane displays a porous surface (Figure 2A). EDX imaging of the membrane (the inset in Figure 2A) shows the uniform distribution of Na element in the membrane, demonstrating the transformation of PAA into PAAS and the uniform distribution of PAAS in the membrane. The top-view environmental SEM image of the wet PVDF/PAAS-g-PVDF blend membrane exhibits a smooth surface without visible

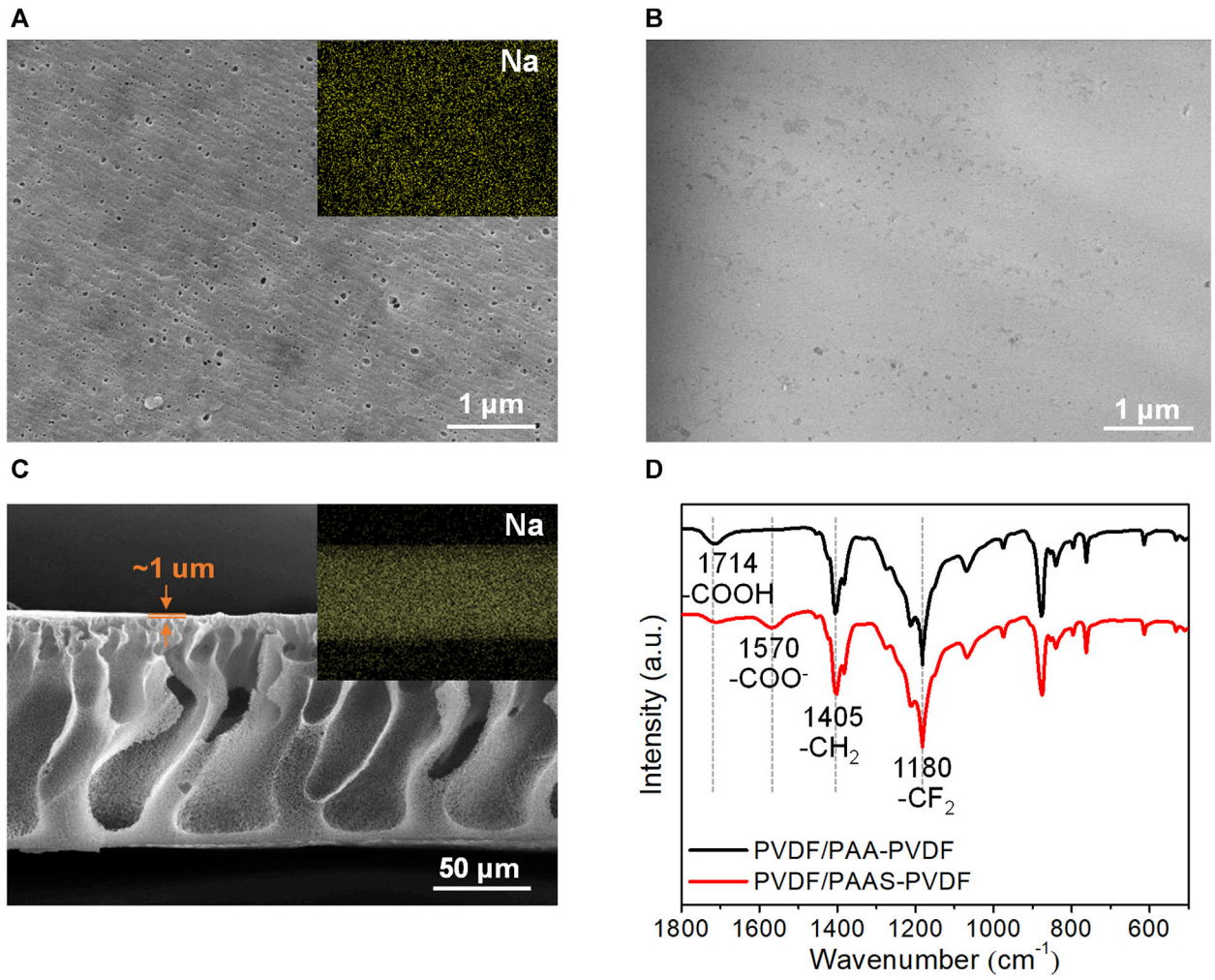

FIGURE 2
Morphology and chemical composition of the PVDF/PAAS-g-PVDF blend membrane. **(A)** Top-view SEM image of the membrane in a dry state and corresponding EDX imaging of Na element. **(B)** Top-view environmental SEM image of the membrane in a wet state. **(C)** Cross-sectional SEM image of the membrane in a dry state and corresponding EDX imaging of Na element. **(D)** ATR-FTIR spectra of the PVDF/PAA-g-PVDF blend membrane and the PVDF/PAAS-g-PVDF blend membrane.

pores (Figure 2B), which is ascribed to the hydration and swelling of PAAS. The cross-sectional SEM image of the dry PVDF/PAAS-g-PVDF blend membrane shows a finger-like pore structure of the membrane (Figure 2C). The thickness of the whole membrane is ~120 μm, and the thickness of the skin layer is ~1 μm. To further confirm the formation of PAAS in the blend membrane, the ATR-FTIR spectra of the PVDF/PAAS-g-PVDF blend membrane and the PVDF/PAA-g-PVDF blend membrane were measured (Figure 2D). In comparison with the PVDF/PAA-g-PVDF blend membrane, the absorption peak at 1714 cm^{-1} which corresponds to the stretching vibration of COOH decreases, and an absorption peak at 1,570 cm^{-1} which corresponds to the stretching vibration of COO^- is observed in the PVDF/PAAS-g-PVDF blend membrane, demonstrating the *in-situ* ionization of PAA into PAAS. The absorption peaks at 1,180 cm^{-1} and 1,405 cm^{-1} are ascribed to the stretching vibration of CF_2 and CH_2 in PVDF, respectively. The atomic percentage of Na and O in the PVDF/PAAS-g-PVDF blend membrane is 0.33% and 1.03%, respectively (Supplementary Figure S1), indicating that ~64% PAA has been transformed into PAAS in the membrane.

3.2 Wettability and anti-oil-fouling property of the blend membrane

Underwater oil adhesive force is critical to evaluate the anti-oil-fouling property of a membrane. As shown in Figure 3, the real-time recorded force-distance curves were plotted according to the dynamic measurement of the underwater crude oil adhesive force of the PVDF/PAAS-g-PVDF blend membrane and the PVDF/PAA-g-PVDF blend membrane. During the measurement, a heavy crude oil droplet was used as the detecting probe to sufficiently contact the membrane surface and then lift up under water. There is no deformation of the crude oil droplet when lifting the oil droplet up from the PVDF/PAAS-g-PVDF blend membrane (Figure 3A). The detected underwater crude oil adhesive force of the PVDF/PAAS-g-PVDF blend membrane is only 1.8 ± 0.1 μN, indicating an excellent anti-oil-adhesive property. In contrast, the crude oil droplet tightly adheres on the PVDF/PAA-g-PVDF blend membrane with obvious deformation when lifting the oil droplet up from the membrane (Figure 3B). The detected underwater crude

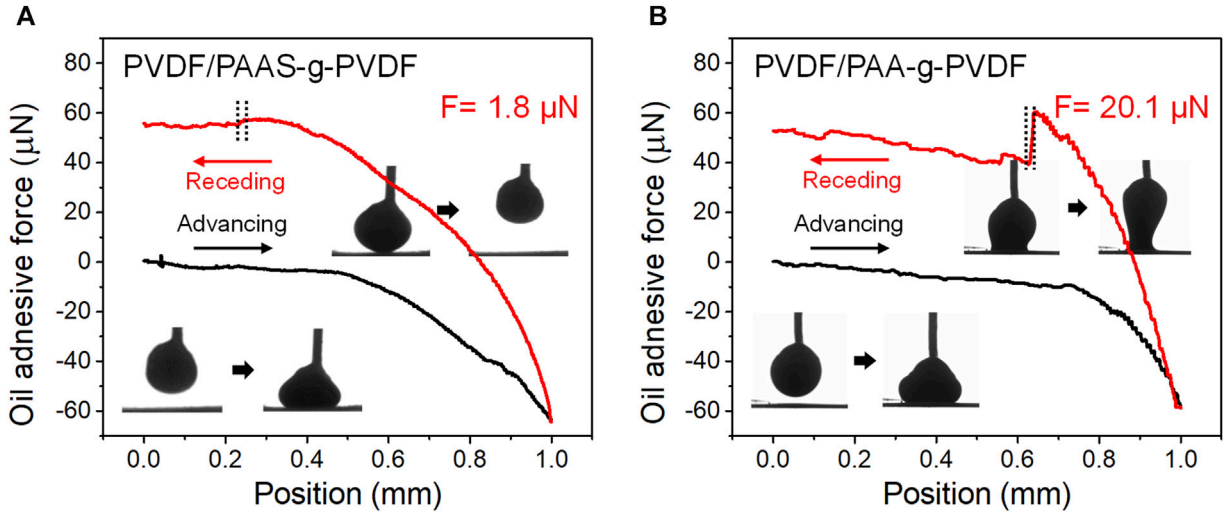

FIGURE 3
Real-time recorded force-distance curves during the dynamic measurements of underwater crude oil adhesive force on **(A)** the PVDF/PAAS-g-PVDF blend membrane and **(B)** the PVDF/PAA-g-PVDF blend membrane. A heavy crude oil droplet (3 μL) was used as the detecting probe.

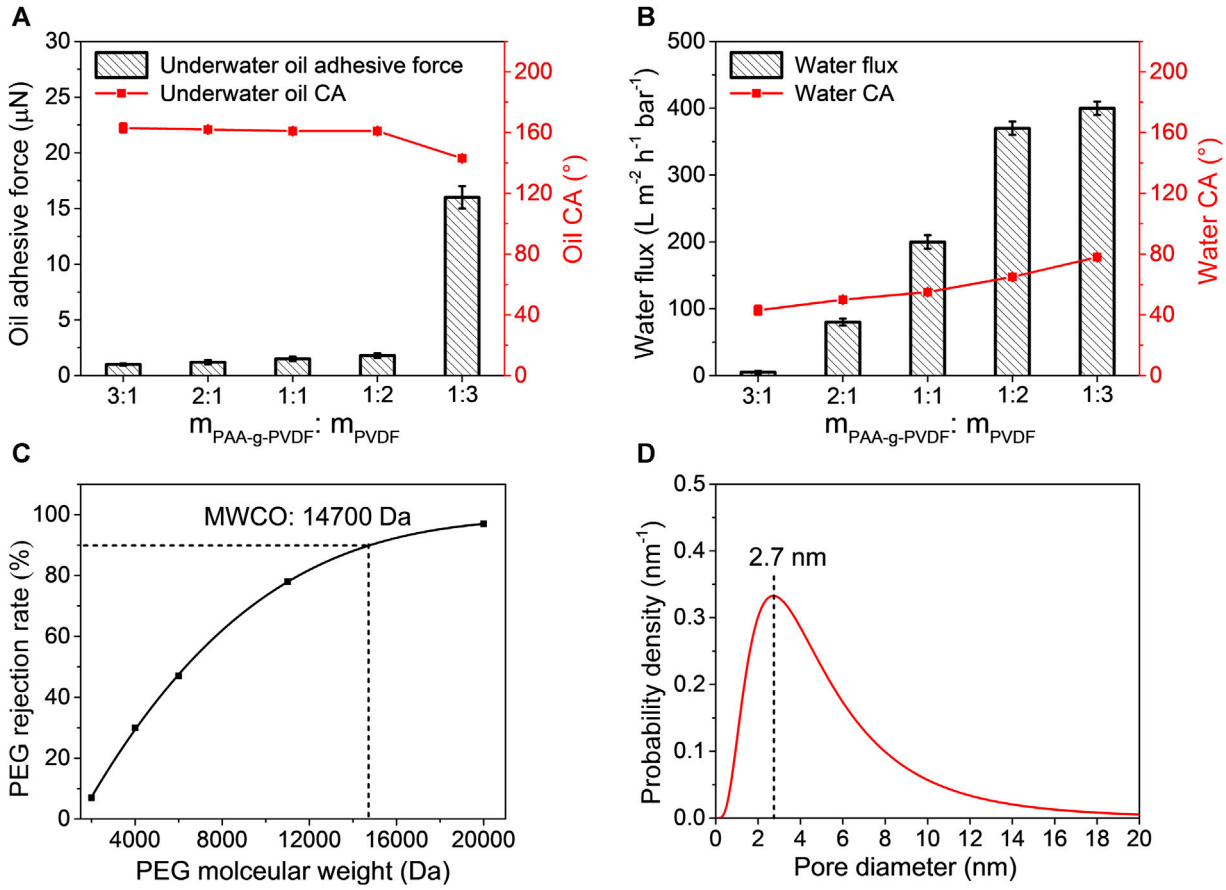

FIGURE 4
(A) Underwater crude oil adhesive force, underwater crude oil CA and **(B)** pure water flux, water CA of the PVDF/PAAS-g-PVDF blend membranes fabricated with different mass ratios of PAA-g-PVDF and PVDF. **(C)** PEG rejection curve and **(D)** pore size distribution of the PVDF/PAAS-g-PVDF blend membrane fabricated with $m_{PAA\text{-}g\text{-}PVDF}$: m_{PVDF} = 1: 2.

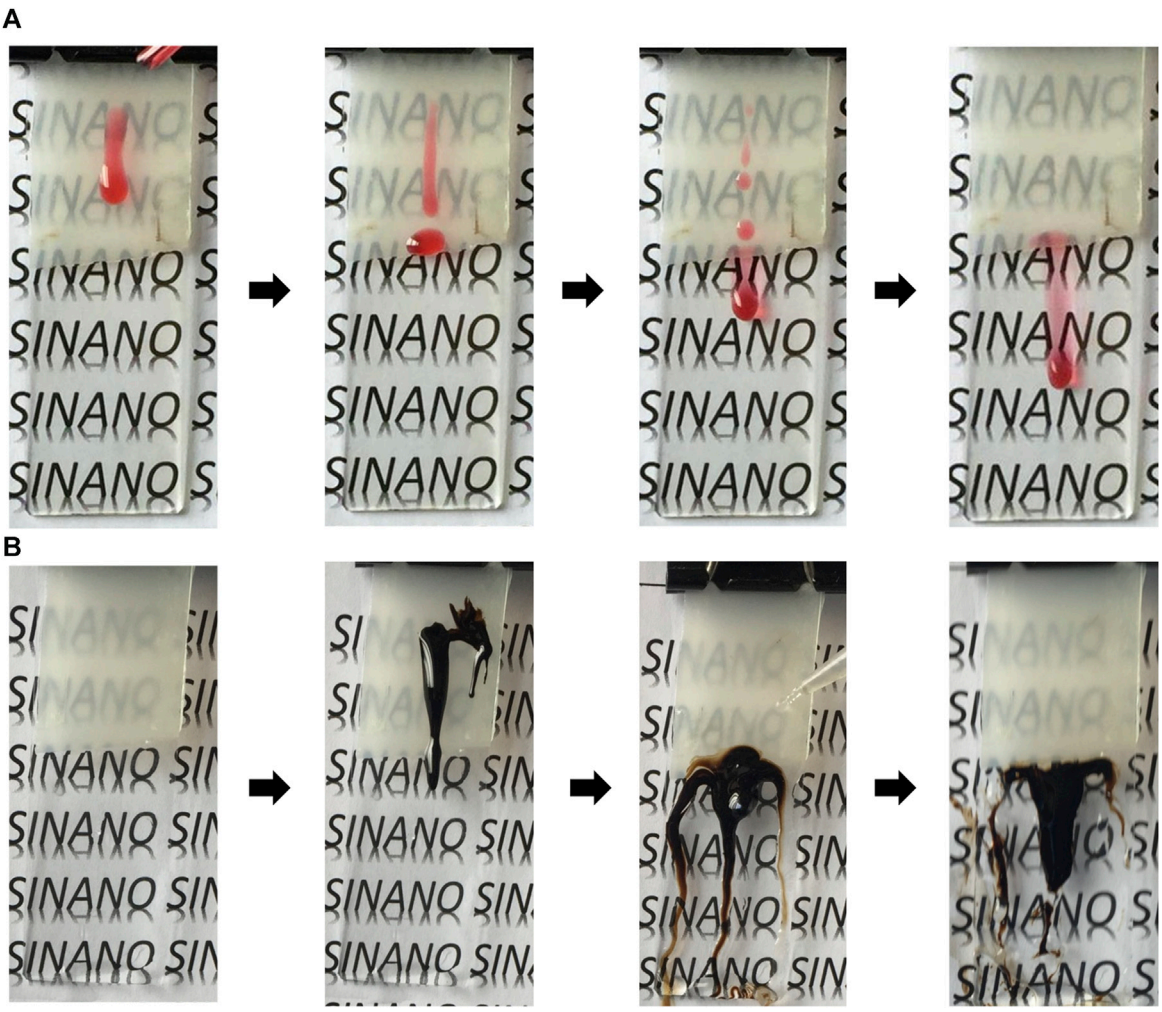

FIGURE 5
Photographs showing the anti-oil-fouling ability test of the PVDF/PAAS-g-PVDF blend membrane for **(A)** soybean oil (dyed red) and **(B)** crude oil.

oil adhesive force of the PVDF/PAA-g-PVDF membrane is as high as 20 ± 0.5 μN. Compared with the PVDF/PAA-g-PVDF blend membrane, the greatly decreased underwater oil adhesive force and superior anti-oil-adhesive property of the PVDF/PAAS-g-PVDF blend membrane is owing to the strong hydration ability of PAAS. The PVDF/PAAS-g-PVDF blend membrane can form a hydration layer on the membrane surface to prevent oil from contacting and adhering. Benefiting from the introduce of PAAS, the PVDF/PAAS-g-PVDF blend membrane also shows the hydrophilicity with the water CA of 65° ± 2°, as well as the underwater superoleophobicity with the crude oil CA of 161° ± 1° and the soybean oil CA of 163° ± 2° (Supplementary Figure S2).

As the easy hydrating and swelling feature of PAAS would result in pore blocking and extremely low water flux of the blend membrane, we investigated the effect of the PAAS content on the wettability and water flux of the PVDF/PAAS-g-PVDF blend membrane. A series of PVDF/PAAS-g-PVDF blend membranes were fabricated with the PAA-g-PVDF: PVDF mass ratios of 3: 1, 2: 1, 1: 1, 1: 2 and 1: 3. The PAAS content in the PVDF/PAAS-g-PVDF blend membrane increases with increasing the PAA-g-PVDF: PVDF mass ratio. As shown in Figure 4A, the underwater crude oil adhesive force of the PVDF/PAAS-g-PVDF blend membrane increases slightly from 1 to 1.8 μN, and the underwater crude oil CA decreases from 163° to 161° with increasing the PAA-g-PVDF: PVDF mass ratio from 3: 1 to 1: 2. Meanwhile, the water CA of the membrane increases from 43° to 65°, and the pure water flux increases from 5 L m^{-2} h^{-1} bar^{-1}–370 L m^{-2} h^{-1} bar^{-1} (Figure 4B). When further increasing the PAA-g-PVDF: PVDF mass ratio to 1: 3, the PVDF/PAAS-g-PVDF blend membrane exhibits high underwater crude oil adhesive force of 16.2 μN and low underwater crude oil CA of 143°, although the membrane shows a pure water flux of 400 L m^{-2} h^{-1} bar^{-1}. Therefore, the PVDF/PAAS-g-PVDF blend membrane fabricated with the PAA-g-PVDF: PVDF mass ratios of 1: 2 is chosen for evaluating the anti-oil-fouling ability and oil/water separation performance in term of its outstanding anti-oil-adhesive property, underwater superoleophobicity, hydrophilicity and high water flux. Effective pore size of this PVDF/PAAS-g-PVDF blend membrane in water was studied according to the rejection rates of PEG with different molecular weights (Figure 4C). From the nonlinearly fitted PEG rejection curve, the molecular weight cut-off (MWCO) of the membrane is 14700 Da, which is defined as the molecular weight at the rejection rate of 90%. Based on a probability density function

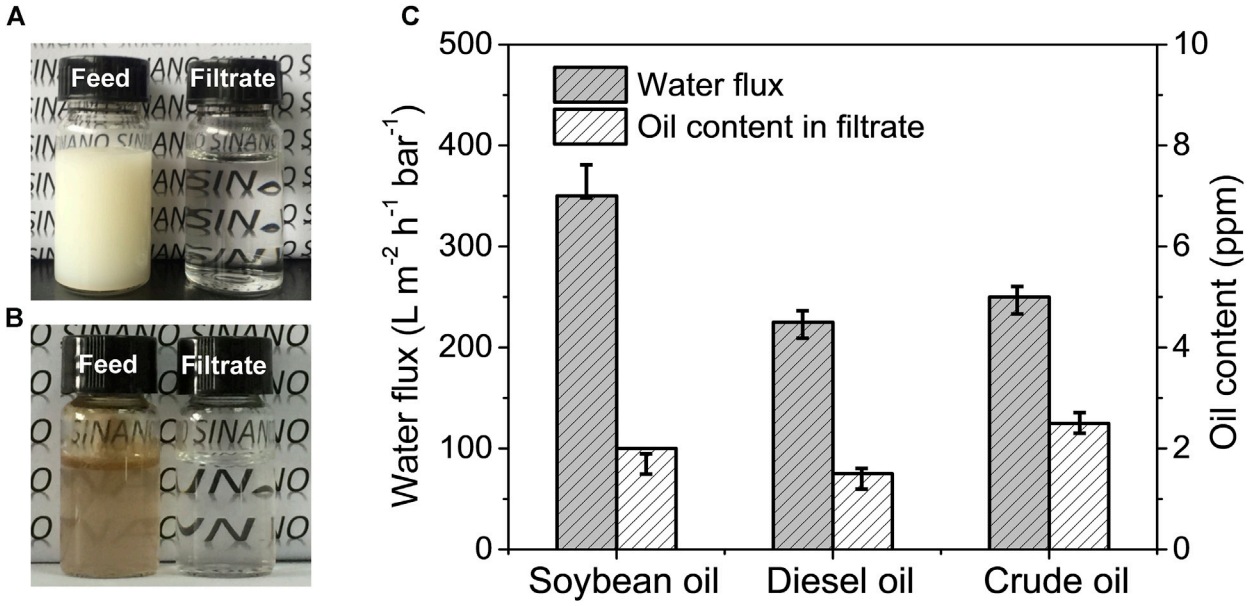

FIGURE 6
Photographs of the emulsion feed and the filtrated water of **(A)** the SDS-stabilized soybean oil-in-water emulsion and **(B)** the SDS-stabilized crude oil-in-water emulsion. **(C)** Water flux and oil content in the filtrate for the separation of the SDS-stabilized oil-in-water emulsions by the PVDF/PAAS-g-PVDF blend membrane.

between the rejection rate and Stokes radius (Lin et al., 2016; Jiang et al., 2018), the mean pore diameter of the membrane is calculated to be 2.7 nm, and the pore diameter distribution is shown in Figure 4D. The PVDF/PAAS-g-PVDF blend membrane is a typical ultrafiltration membrane.

The anti-oil-fouling property of the PVDF/PAAS-g-PVDF blend membrane was also tested. As shown in Figure 5, the half of a glass plate was covered by the wet PVDF/PAAS-g-PVDF blend membrane and vertically placed. The light oil like soybean oil and the viscous oil like heavy crude oil were chosen as the oil contaminants to foul the membrane, respectively. When the soybean oil was dropped on the membrane, the soybean oil slid off from the membrane spontaneously without leaving any trace (Figure 5A). When the heavy crude oil was used to foul the membrane, the crude oil shed off from the membrane immediately once the membrane was rinsed by a bunch of water (Figure 5B). These results demonstrate the outstanding oil-repellent and anti-oil-fouling property of the PVDF/PAAS-g-PVDF blend membrane for both the light oil and the viscous oil. The membrane can be easily cleaned by water washing when the membrane is fouled by oil.

3.3 Oil-in-water emulsion separation and cycling performance

A series of SDS-stabilized oil-in-water emulsions including soybean oil-, diesel oil- and crude oil-in-water emulsion were prepared and filtrated through the PVDF/PAAS-g-PVDF blend membrane under a transmembrane pressure of 1 bar to carry out the separation process, respectively. The optical images of the soybean oil-in-water emulsion and the crude oil-in-water emulsion before and after separation are shown in Figures 6A, B. The milky white soybean oil-in-water emulsion and the turbid brown crude oil-in-water emulsion turn to be transparent clear after one-step separation by the PVDF/PAAS-g-PVDF blend membrane. All the oil contents in the filtrates are below 3 ppm for the three oil-in-water emulsions, which is equivalent to the separation efficiency above 99.97% (Figure 6C). These results indicate that the PVDF/PAAS-g-PVDF blend membrane can remove nearly all of the oil droplets from the oil-in-water emulsion, and owns ultrahigh separation efficiency. The high oil rejection of the PVDF/PAAS-g-PVDF blend membrane is benefited from its superior oil-repellent property and small effective pore size. The PVDF/PAAS-g-PVDF blend membrane also exhibits high water flux during the separation of the three oil-in-water emulsions: $350 \pm 30\ L\ m^{-2}\ h^{-1}\ bar^{-1}$ for soybean oil-in-water emulsion, $225 \pm 20\ L\ m^{-2}\ h^{-1}\ bar^{-1}$ for diesel oil-in-water emulsion, and $250 \pm 20\ L\ m^{-2}\ h^{-1}\ bar^{-1}$ for crude oil-in-water emulsion, respectively (Figure 6C).

To study the cycling performance of the PVDF/PAAS-g-PVDF blend membrane, the water flux during several separation cycles of the SDS-stabilized crude oil-in-water emulsion by the membrane was monitored. Same tests were carried out on the PVDF/PAA-g-PVDF blend membrane as a contrast. Figure 7A summarizes the alternating water flux of the membranes between filtrating pure water and filtrating the crude oil-in-water emulsion. In the first separation cycle, the PVDF/PAAS-g-PVDF blend membrane exhibits an initial pure water flux of $370 \pm 10\ L\ m^{-2}\ h^{-1}\ bar^{-1}$. When the crude oil-in-water emulsion is switched to be filtrated through the membrane, the water flux decreases and stabilizes at $250 \pm 20\ L\ m^{-2}\ h^{-1}\ bar^{-1}$ with a flux decline ratio *DR* of 32.4% (Figure 7B). After water washing, the pure water flux of the membrane recovers to $320 \pm 10\ L\ m^{-2}\ h^{-1}\ bar^{-1}$ in the second separation cycle with a flux recovery ratio *FRR* of 86.5%. It means that the water flux of the PVDF/PAA-g-PVDF blend membrane can be easily recovered by hydraulic flushing. Generally, membrane fouling can

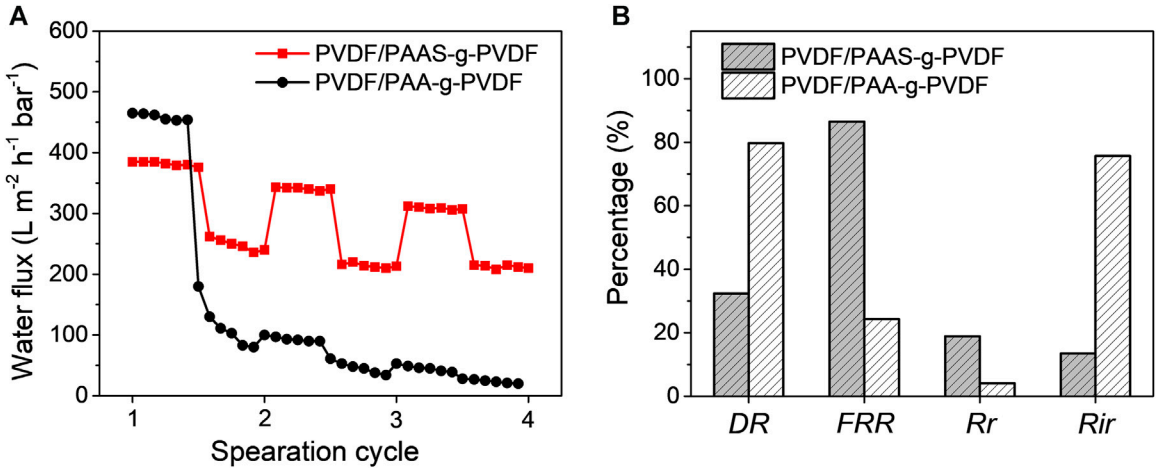

FIGURE 7
(A) Water flux variation of the PVDF/PAAS-g-PVDF blend membrane and the PVDF/PAA-g-PVDF blend membrane during three separation cycles of the SDS-stabilized crude oil-in-water emulsion. **(B)** Corresponding parameters for evaluating the antifouling ability of the membranes.

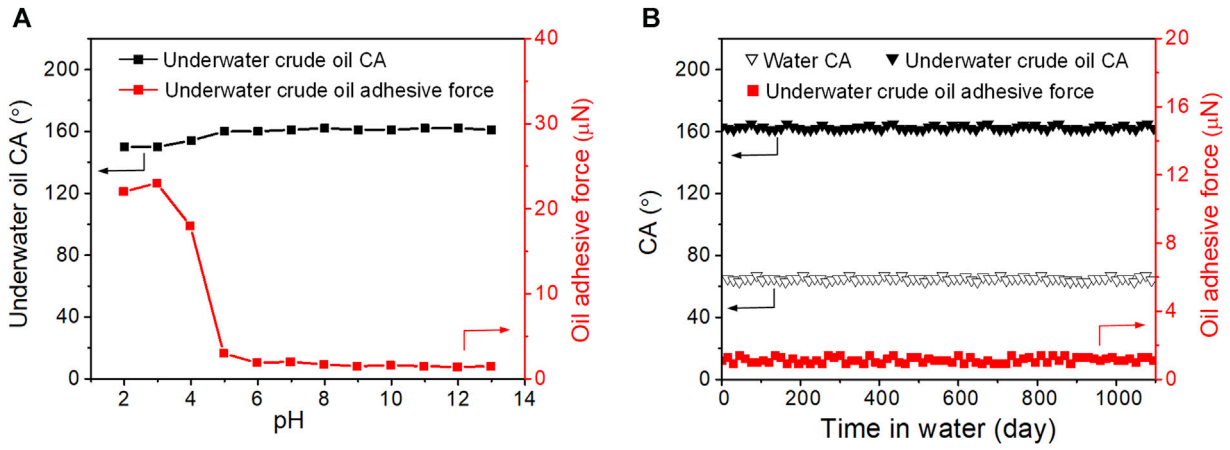

FIGURE 8
(A) Variation of underwater crude oil CA and underwater crude oil adhesive force of the PVDF/PAAS-g-PVDF blend membrane under different pH environments. **(B)** Variation of water CA, underwater crude oil CA and underwater crude oil adhesive force of the PVDF/PAAS-g-PVDF blend membrane in water (pH = 7) for 1,100 days.

be defined as reversible and irreversible fouling. Reversible fouling is caused by weak adhesion of the oil foulants which can be removed by hydraulic washing. Irreversible fouling corresponds to strong adhesion of the oil foulants or the oil foulants entrapped in the membrane pores which cannot be physically removed. The reversible fouling ratio *Rr* is 18.9%, and the irreversible fouling ratio *Rir* is 13.5% for the PVDF/PAAS-g-PVDF blend membrane according to the flux variation. As a contrast, the water flux of the PVDF/PAA-g-PVDF blend membrane decreases from 475 ± 10 L m^{-2} h^{-1} bar^{-1} to 75 ± 5 L m^{-2} h^{-1} bar^{-1} when filtrating the same crude oil-in-water emulsion. After the same water washing, the pure water flux can only recover to 90 ± 5 L m^{-2} h^{-1} bar^{-1} in the second separation cycle. The flux decline ratio *DR* is as high as 84.2%, the flux recovery ratio *FRR* is only 18.9%, the reversible fouling ratio *Rr* is 3.2%, and the irreversible fouling ratio *Rir* is 81.0% for the PVDF/PAA-g-PVDF blend membrane. What's more, the PVDF/PAA-g-PVDF blend membrane exhibits the always decreased water flux to nearly zero when filtrating the crude oil-in-water emulsion in the second and the third separation cycle. These results demonstrate the excellent antifouling and cycling performance of the PVDF/PAAS-g-PVDF blend membrane, which is of vital importance to achieve long-term efficient separation of the oil-in-water emulsions.

3.4 Stability of the blend membrane

The mechanical strength of the PVDF/PAAS-g-PVDF blend membrane in the wet state was measured by a universal testing machine, and the same measurement was carried out on the PVDF/PAA-g-PVDF blend membrane as a contrast. As shown in Supplementary Figure S3, the two membranes show the similar tensile

strength of ~1 MPa. The PVDF/PAAS-g-PVDF blend membrane exhibits the engineering strain of ~82% which is almost two times of the PVDF/PAA-g-PVDF blend membrane. It indicates that the PVDF/PAAS-g-PVDF blend membrane has better tensile breaking resistance than the PVDF/PAA-g-PVDF blend membrane owing to the good extensibility of the hydrated PAAS. In view of the easy deformation feature of PAAS under a high pressure, the pore size and separation performance of the PVDF/PAAS-g-PVDF blend membrane may be influenced by the transmembrane pressure. We investigated the performance stability of the PVDF/PAAS-g-PVDF blend membrane under different transmembrane pressures during the separation of the SDS-stabilized soybean oil-in-water emulsion. The membrane shows stable water flux of 335–350 L m^{-2} h^{-1} bar^{-1} under the transmembrane pressures of 1–3 bar (Supplementary Figure S4), revealing the well-maintained pore size. When further increasing the transmembrane pressure to 4 bar, the water flux decreases to 270 L m^{-2} h^{-1} bar^{-1} on account of the compressed membrane pores under such a high pressure. Under the transmembrane pressures of 1–4 bar, the oil content in the filtrate after separation was always below 3 ppm, indicating the stable separation efficiency of the membrane. The pH stability of the PVDF/PAAS-g-PVDF blend membrane was also evaluated by recording its underwater crude oil CA and underwater crude oil adhesive force after immersing the membrane in water with different pH from 2 to 13 for 10 days, respectively. Under the pH from 5 to 12, the membrane exhibits stable low-oil-adhesive underwater superoleophobicity with the underwater crude oil CA above 160° and crude oil adhesive force below 2 μN (Figure 8A). When the pH is below 4, the underwater crude oil CA decreases to 153°, and the crude oil adhesive force increases sharply to 20 μN. This is ascribed to the transformation of PAAS to PAA in the acidic environment, as the acid dissociation constant of PAA is 4.2–4.5. Therefore, the PVDF/PAAS-g-PVDF blend membrane can maintain the outstanding anti-oil-fouling ability under a wide pH range of 5–12.

Restraining the release of the hydrophilic additives from the membranes to water, and endowing the membranes with high stability for long-term use is critically important for developing the blend membranes. In order to evaluate the long-term stability of the PVDF/PAAS-g-PVDF blend membrane, the water CA, underwater crude oil CA and underwater crude oil adhesive force of the membrane were continuously monitored for 1,100 days. During the test, the membrane was immersed in water with the pH of about 7, and the wettability parameters were recorded every 15 days. As shown in Figure 8B, the PVDF/PAAS-g-PVDF blend membrane maintains the hydrophilicity with water CA below 70°, and the underwater superoleophobicity with crude oil CA above 160°, as well as the low-oil-adhesive property with underwater crude oil adhesive force below 2 μN during the whole test period. After the test, the surface morphology and chemical composition of the PVDF/PAAS-g-PVDF blend membrane was nearly unchanged (Supplementary Figure S5), indicating that the hydrophilic PAAS is stably blended in the membrane without obvious release. It is because of the strong interaction between the PAAS-g-PVDF additive and the PVDF matrix. These results indicate the high stability of the PVDF/PAAS-g-PVDF blend membrane for long-term use.

4 Conclusion

In this work, we proposed a facile method to introduce the strong hydrophilic PAAS in PVDF to fabricate the hydrophilic, underwater low-oil-adhesive superoleophobic and anti-oil-fouling blend ultrafiltration membrane. PAA-g-PVDF was used as the additive precursor to blend with the PVDF matrix to form the uniform PVDF/PAA-g-PVDF blend membrane via the nonsolvent-induced phase inversion. Then PAA in the blend membrane was *in situ* ionized to PAAS to endow the final PVDF/PAAS-PVDF blend membrane with strong hydration ability and superior anti-oil-fouling property. The wettability and water permeation flux of the PVDF/PAAS-g-PVDF blend membrane were optimized by regulating the mass ratio of PVDF and PAA-g-PVDF. The PVDF/PAAS-g-PVDF blend membrane achieved efficient separation of multiple emulsifier-stabilized oil-in-water emulsions even including the viscous crude oil-in-water emulsion, with ultrahigh separation efficiency of 99.97%, high water flux of 350 L m^{-2} h^{-1} bar^{-1}, as well as good cycling performance. The blend membrane also exhibited long-term stability lasting for 1,100 days due to the strong interaction between the PAAS-g-PVDF additive and the PVDF matrix. The blend membrane with the outstanding anti-oil-fouling property had a great potential for prolonged separation of real emulsified oily wastewater in a large scale.

Data availability statement

The original contributions presented in the study are included in the article/Supplementary Material, further inquiries can be directed to the corresponding authors.

Author contributions

SG: Conceptualization, Data curation, Formal Analysis, Funding acquisition, Investigation, Methodology, Writing–original draft, Supervision. PL: Data curation, Formal Analysis, Methodology, Writing–original draft. JJ: Conceptualization, Funding acquisition, Supervision, Writing–review and editing.

Funding

The author(s) declare financial support was received for the research, authorship, and/or publication of this article. This work was financially supported by the National Natural Science Foundation of China (21988102, 22105219), the National Key Research and Development Program of China (2022YFB3804901, 2022YFB3804900, 2019YFA0705800), the Natural Science Foundation of Jiangsu Province (BK20210132), the Key Research and Development Plan of Jiangsu Province (BE2022056), the Gusu's Young Leading Talent Program (ZXL2022461) and the Doctoral

Program of Innovation and Entrepreneurship in Jiangsu Province (JSSCBS20211415).

Acknowledgments

We acknowledge the kind support of the PAA-g-PVDF powders by Prof. Jingye Li from Shanghai Normal University.

Conflict of interest

The authors declare that the research was conducted in the absence of any commercial or financial relationships that could be construed as a potential conflict of interest.

Publisher's note

Supplementary material

The Supplementary Material for this article can be found online at: https://www.frontiersin.org/articles/10.3389/frmst.2024.1355773/full#supplementary-material

References

Aurell, J., and Gullett, B. K. (2010). Aerostat sampling of PCDD/PCDF emissions from the Gulf oil spill *in situ* burns. *Environ. Sci. Technol.* 44, 9431–9437. doi:10.1021/es103554y

Chang, Q., Zhou, J.-E., Wang, Y., Liang, J., Zhang, X., Cerneaux, S., et al. (2014). Application of ceramic microfiltration membrane modified by nano-TiO_2 coating in separation of a stable oil-in-water emulsion. *J. Membr. Sci.* 456, 128–133. doi:10.1016/j.memsci.2014.01.029

Chen, P., and Xu, Z. (2013). Mineral-coated polymer membranes with superhydrophilicity and underwater superoleophobicity for effective oil/water separation. *Sci. Rep.* 3, 2776. doi:10.1038/srep02776

Chen, Y., Wei, M., and Wang, Y. (2016). Upgrading polysulfone ultrafiltration membranes by blending with amphiphilic block copolymers: beyond surface segregation. *J. Membr. Sci.* 505, 53–60. doi:10.1016/j.memsci.2016.01.030

Choi, J.-H., Jegal, J., and Kim, W.-N. (2006). Fabrication and characterization of multi-walled carbon nanotubes/polymer blend membranes. *J. Membr. Sci.* 284, 406–415. doi:10.1016/j.memsci.2006.08.013

Chu, Z., Feng, Y., and Seeger, S. (2015). Oil/water separation with selective superantiwetting/superwetting surface materials. *Angew. Chem. Int. Ed.* 54, 2328–2338. doi:10.1002/anie.201405785

Dong, D., Zhu, Y., Fang, W., Ji, M., Wang, A., Gao, S., et al. (2022). Double-defense design of super-anti-fouling membranes for oil/water emulsion separation. *Adv. Funct. Mater.* 32, 2113247. doi:10.1002/adfm.202113247

Elimelech, M., and Phillip, W. A. (2011). The future of seawater desalination: energy, technology, and the environment. *Science* 333, 712–717. doi:10.1126/science.1200488

Gao, S., Chen, J., Zheng, Y., Wang, A., Dong, D., Zhu, Y., et al. (2022). Gradient adhesive hydrogel decorated superhydrophilic membranes for ultra-stable oil/water separation. *Adv. Funct. Mater.* 32, 2205990. doi:10.1002/adfm.202205990

Gao, S., Sun, J., Liu, P., Zhang, F., Zhang, W., Yuan, S., et al. (2016). A robust polyionized hydrogel with an unprecedented underwater anti-crude-oil-adhesion property. *Adv. Mater.* 28, 5307–5314. doi:10.1002/adma.201600417

Gao, S., Zhu, Y., Zhang, F., and Jin, J. (2015). Superwetting polymer-decorated SWCNT composite ultrathin films for ultrafast separation of oil-in-water nanoemulsions. *J. Mater. Chem. A* 3, 2895–2902. doi:10.1039/C4TA05624H

Geng, H., Zhong, Q.-Z., Li, J., Lin, Z., Cui, J., Caruso, F., et al. (2022). Metal ion-directed functional metal-phenolic materials. *Chem. Rev.* 122, 11432–11473. doi:10.1021/acs.chemrev.1c01042

Jiang, G., Zhang, S., Zhu, Y., Gao, S., Jin, H., Luo, L., et al. (2018). Hydrogel-embedded tight ultrafiltration membrane with superior anti-dye-fouling property for low-pressure driven molecule separation. *J. Mater. Chem. A* 6, 2927–2934. doi:10.1039/C7TA09898G

Kang, G., and Cao, Y. (2014). Application and modification of poly (vinylidene fluoride)(PVDF) membranes-a review. *J. Membr. Sci.* 463, 145–165. doi:10.1016/j.memsci.2014.03.055

Lin, J., Ye, W., Baltaru, M. C., Tang, Y. P., Bernstein, N. J., Gao, P., et al. (2016). Tight ultrafiltration membranes for enhanced separation of dyes and Na_2SO_4 during textile wastewater treatment. *J. Membr. Sci.* 514, 217–228. doi:10.1016/j.memsci.2016.04.057

Liu, F., Hashim, N. A., Liu, Y., Abed, M. R. M., and Li, K. (2011). Progress in the production and modification of PVDF membranes. *J. Membr. Sci.* 375, 1–27. doi:10.1016/j.memsci.2011.03.014

Oki, T., and Kanae, S. (2006). Global hydrological cycles and world water resources. *Science* 313, 1068–1072. doi:10.1126/science.1128845

Rana, D., and Matsuura, T. (2010). Surface modifications for antifouling membranes. *Chem. Rev.* 110, 2448–2471. doi:10.1021/cr800208y

Shi, Q., Su, Y., Zhao, W., Li, C., Hu, Y., Jiang, Z., et al. (2008). Zwitterionic polyethersulfone ultrafiltration membrane with superior antifouling property. *J. Membr. Sci.* 319, 271–278. doi:10.1016/j.memsci.2008.03.047

Tao, M., Xue, L., Liu, F., and Jiang, L. (2014). An intelligent superwetting PVDF membrane showing switchable transport performance for oil/water separation. *Adv. Mater.* 26, 2943–2948. doi:10.1002/adma.201305112

Wang, A., Zhu, Y., Fang, W., Gao, S., and Jin, J. (2023). Zero-oil-fouling membrane with high coverage of grafted zwitterionic polymer for separation of oil-in-water emulsions. *Small Methods*, 2300247. doi:10.1002/smtd.202300247

Wang, B., Liang, W., Guo, Z., and Liu, W. (2015). Biomimetic super-lyophobic and super-lyophilic materials applied for oil/water separation: a new strategy beyond nature. *Chem. Soc. Rev.* 44, 336–361. doi:10.1039/C4CS00220B

Yang, C., Long, M., Ding, C., Zhang, R., Zhang, S., Yuan, J., et al. (2022). Antifouling graphene oxide membranes for oil-water separation via hydrophobic chain engineering. *Nat. Commun.* 13, 7334. doi:10.1038/s41467-022-35105-8

Yang, H., Pi, J., Liao, K., Huang, H., Wu, Q., Huang, X., et al. (2014). Silica-decorated polypropylene microfiltration membranes with a mussel-inspired intermediate layer for oil-in-water emulsion separation. *ACS Appl. Mater. Interfaces* 6, 12566–12572. doi:10.1021/am502490j

Yang, X., Martinson, A., Elam, J. W., Shao, L., and Darling, S. (2021). Water treatment based on atomically engineered materials: atomic layer deposition and beyond. *Matter* 4, 3515–3548. doi:10.1016/j.matt.2021.09.005

Yang, X., Wen, Y., Li, Y., Yan, L., Tang, C., Ma, J., et al. (2023). Engineering *in situ* catalytic cleaning membrane via prebiotic-chemistry-inspired mineralization. *Adv. Mater.* 35, 2306626. doi:10.1002/adma.202306626

Zhang, F., Zhang, W., Shi, Z., Wang, D., Jin, J., and Jiang, L. (2013b). Nanowire-haired inorganic membranes with superhydrophilicity and underwater ultralow adhesive superoleophobicity for high-efficiency oil/water separation. *Adv. Mater.* 25, 4192–4198. doi:10.1002/adma.201301480

Zhang, L., Zhong, Y., Cha, D., and Wang, P. (2013a). A self-cleaning underwater superoleophobic mesh for oil-water separation. *Sci. Rep.* 3, 2326. doi:10.1038/srep02326

Zhang, W., Zhu, Y., Liu, X., Wang, D., Li, J., Jiang, L., et al. (2014). Salt-induced fabrication of superhydrophilic and underwater superoleophobic PAA-g-PVDF membranes for effective separation of oil-in-water emulsions. *Angew. Chem. Int. Ed.* 53, 856–860. doi:10.1002/anie.201308183

Zhu, Y., Wang, D., Jiang, L., and Jin, J. (2014). Recent progress in developing advanced membranes for emulsified oil/water separation. *NPG Asia Mater* 6, e101. doi:10.1038/am.2014.23